Heliyon 10 (2024) e25201

Contents lists available at ScienceDirect

Heliyon

journal homepage: www.cell.com/heliyon

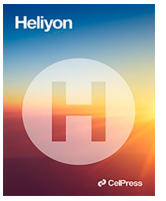

Research article

Inactivation of hepatitis A virus, feline calicivirus, and Tulane virus on Formica coupons using ultraviolet light technologies

E. Corson [a], B. Pendyala [b], A. Patras [b], D.H. D'Souza [a,*]

[a] Department of Food Science, 2600 River Drive, University of Tennessee, Knoxville, TN 37996, USA
[b] Department of Food and Animal Sciences, Tennessee State University, Nashville, Tennessee 37209, USA

ARTICLE INFO

Keywords:
Hepatitis A virus
Feline calicivirus
Tulane virus
Contact surface
Ultraviolet light emitting diode technology

ABSTRACT

Contaminated fomites can lead to hepatitis A virus (HAV) and human norovirus (HuNoV) disease outbreaks. Improved decontamination methods that are user-friendly, cost-effective, and waterless are being researched for sustainability. Traditional ultraviolet light (UV–C) technologies though effective for surface decontamination have drawbacks, using mercury lamps, that pose user-safety risk and environmental hazards. Therefore, UV-C light emitting diode (LED) systems are being designed for delivering required antiviral doses. The objective of this research was to determine the ability of UV-C LED (279 nm) systems to inactivate HuNoV surrogates, feline calicivirus (FCV–F9) and Tulane virus (TV), and HAV on Formica coupons in comparison to UV-C (254 nm) systems. FCV-F9 (~6 log PFU/mL), TV (~7 log PFU/mL), or HAV (~6 log PFU/mL) at 100 μL were surface-spread on sterile Formica coupons (3 × 3 cm^2), air-dried, and treated for up to 2.5 min with both systems. Each experiment was replicated thrice. Recovered infectious plaque counts were statistically analyzed using mixed model analysis of variance. FCV-F9, TV, and HAV showed D_{10} values of 23.37 ± 0.91 mJ/cm^2, 16.32 ± 3.6 mJ/cm^2, and 12.39 ± 0.70 mJ/cm^2 using 279 nm UV-C LED, respectively and D_{10} values of 9.97 ± 2.44 mJ/cm^2, 6.83 ± 1.13 mJ/cm^2 and 12.40 ± 1.15 mJ/cm^2, respectively with 254 nm UV-C. Higher 279 nm UV-C LED doses were required to cause HuNoV surrogate reduction than 254 nm UV-C, except similar doses with both systems were needed for HAV inactivation on Formica surfaces. It remains critical to measure UV intensity of optical sources and optimize exposure times for desired log reduction on surfaces.

1. Introduction

Foodborne human noroviral (HuNoV) and hepatitis A virus (HAV) outbreaks continue to occur worldwide, including the 2022 HuNoV outbreak involving raw oysters and the 2023 HAV outbreak involving frozen strawberries in the United States [1,2]. Improved sustainable and cost-effective approaches need to be developed and optimized to control these pathogens in the food environment. HuNoV outbreaks continue to emerge with evolving virulent strains that are capable of causing death in the elderly and immunocompromised and those with co-morbidities may be at higher risk, with an estimated 685 million cases reported annually on a global level [3]. While some genogroups of HuNoV have been cultivated in the lab, their titers are not high enough to accurately determine parameters for optimal inactivation [4–7]. Therefore, cultivable HuNoV surrogates including the single-stranded RNA coliphage MS2,

* Corresponding author.
E-mail address: ddsouza@utk.edu (D.H. D'Souza).

https://doi.org/10.1016/j.heliyon.2024.e25201
Received 29 September 2023; Received in revised form 4 December 2023; Accepted 23 January 2024
Available online 28 January 2024

feline calicivirus (FCV–F9), murine norovirus (MNV-1), Tulane virus (TV) and porcine sapovirus continue to be used [4]. Additionally, HAV is another foodborne virus of human health concern that results in severe disease symptoms that last for more than a month [8]. Therefore, improved decontamination strategies are needed to further prevent viral transmission in the food environment.

Ultraviolet light (UV–C at 200–280 nm) technology is recognized as a promising decontamination approach associated with its low cost and low energy consumption [9,10]. Furthermore, UV-C lamps have been approved by the U.S. Food and Drug Administration (US FDA) for surface decontamination of food products to control surface microorganisms [11]. However, for optimal inactivation, the viral target should directly receive an adequate amount of germicidal light (fluence) that can be controlled by varying exposure time [12]. UV light is found to be most effective in the 200–300 nm range, that includes the entire UV-C light range and a part of the UV-B light range [12]. UV-C ranging from 250 to 280 nm is normally used to disinfect water, cooking utensils, and liquid foods [13,14]. Typically, the UV-C light resistance is calculated using the decimal reduction dose (D, expressed in mJ/cm^2) together with the sensitivity of the target virus in the applicable wavelength of light [12].

There are reports in literature on the UV-C inactivation of viruses in fluid suspensions, though viral inactivation on Formica surfaces found in food environments have not been reported. Studies with inactivation on contact surfaces have mainly been conducted using stainless steel and plastic surfaces [14–17]. MNV-1 on stainless steel discs was reported to be reduced by 3 log PFU after 5 min treatment with UV-C at 254 nm, but the calculated dose was not reported in this study [15]. Park et al. [14], showed that 1–2 log PFU reductions of HAV on stainless steel surfaces were observed after treatment with 60–120 mJ/cm^2 of UV-C at 254 nm, with >2 log (PFU) reductions (>99 %) only after treatments with 180 mJ/cm^2 of UV-C, while >2 log (PFU) reductions (>99 %) were observed for MNV-1 on stainless steel coupons, after treatment with 40 mW s/cm^2 of UV-C. This study reported the D-value for MNV-1 to be 33.5 mJ/cm^2 and HAV to be 55.5 mJ/cm^2 [14]. Tailing was observed during inactivation of both these tested viruses using UV-C at 254 nm suggesting the increased exposure time would not cause a proportional increase in inactivation [18]. Therefore, pulsed UV light at 60 mJ/cm^2 and 91 mJ/cm^2 was used that resulted in close to 5 log reduction of HAV and MNV-1 on stainless steel and PVC surfaces [16,17], though this technology is reported to be more expensive than traditional continuous UV-C treatments [19]. It is also important to note that the inactivation by UV-C is theoretically and typically favored on stainless steel surfaces due to the low degree of shielding [18].

Another study showed that 254 nm UV-C treatments of 5-mL suspensions of MNV-1 at 8 log PFU/mL, FCV-F9 at 8.5 log PFU/mL, and MS2 at 10 log PFU/mL on petri dishes resulted in 4 log reduction at fluencies of 29, 25, and 70 mJ/cm^2, respectively [20]. TV at 250 μL in 6 well culture plates was reported to be inactivated to non-detectable levels (>4 D reduction) after UV-C treatment at 254 nm with 60–70 mJ/cm^2 [4]. Treatments of FCV-F9 suspended in PBS in a Petri dish with 253.4 nm UV-C and 125 mJ/cm^2 resulted in a >2 log PFU/mL reduction, while HAV was decreased by > 4 log PFU/mL with the same treatment [21]. However, the main disadvantage with inactivation using UV-C light is its low penetrability, the need for the UV-C to have direct exposure to the target and the use of mercury lamps that can pose a risk to the user and the environment, with a relatively low shelf-life [11,22,23].

Alternatively, UV-C LED lights are being designed to overcome the drawbacks of traditional UV-C systems that are robust, durable, and inexpensive with low heat emission, wavelength diversity, low energy demand, that do not need warm up time, and are mercury free, with no hazardous waste generation [24]. These UV-LED systems are built from semiconductor materials, with analogous structures to the visible light LEDs, that emit light upon application of an electrical current [25,26]. Researchers treated 100 μL of SARS-CoV-2 suspension at 3.16×10^6 $TCID_{50}$ (50 % tissue culture infective dose)/mL held in a Petri dish and covered with a quartz coverslip, with UVC-LED irradiance at 280 ± 5 nm (using a 1000 mW LED module) at different heights (10, 20, 30, and 50 cm) for different times (2–60 s) and found that a ≥ 99.99 % viral reduction was obtained after treatment for 30 s at 50 cm, 20 s at 30 cm, 10 s at 20 cm, and 2 s at 10 cm [27]. They reported that a UV dose of >10 mJ/cm^2 caused reduction of 99.99 %, which is optimal for SARS-CoV-2 (an enveloped virus) eradication [27].

Data on inactivation of viruses (other than recent SARS-CoV-2 data) on surfaces with UV-LED systems are also lacking. Most of the published literature has focused on the use of UV-LED in liquid and aerosolized systems with bacteriophages, foodborne bacteria and fungi [28,29]. Coconut water (5 mL, pH = 4.86, 6.2°Brix) treated with UV-LED at 255 nm was shown to inactivate *E. coli* ATCC 8739 by 6.2 log CFU/mL, *Salmonella eneterica* ATCC 13314 by 6.3 log CFU/mL, and *L. monocytogenes* ATCC 19111 by 5.6 log CFU/mL [24,27]. UV-LED treatments of a carrot, grape, ginger, lemon, and carob (0.02 mL, pH = 4.01, 7.8°Brix) beverage mix resulted in >4 log CFU/mL reduction of *E. coli* K12 and reduction of mesophilic bacteria by 2.59 log CFU/mL with 280/365 nm wavelength combinations [26,30].

The mechanism of inactivation by UV-C is dependent on the target virus (depending on nucleic acid content and composition, envelope, and protein and UV chromophore content and structure) and the UV wavelength [26,31]. UV-C at 254 nm is reported to inactivate RNA viruses by damaging nucleic acids, by forming pyrimidine dimers, uridine hydrates, and thus preventing replication [32,33]. Other research results suggest that using UV-C at 210–240 nm, damage to RNA occurs due to protein–RNA cross-linking or energy transfer from proteins to RNA [12,18,26], and theoretically at 279 nm damage to protein and protein-RNA structures can also occur. UV treatments of Tulane virus showed decreased host receptor binding and mutagenized its genome, while UV treatment at 220 nm allowed RV-host receptor interaction but prevented replication of the genome, thus indicating that varied virion components were targeted, namely their genome and viral capsid [34].

Thus, UV-C LED is a novel promising approach for broad-spectrum inactivation and routine decontamination of surfaces found in food environments that needs to be further investigated. Therefore, the aim of this study was to determine the ability of a UV-C LED light (peak wavelength at 279 nm) system to inactivate HAV and the cultivable HuNoV surrogates (FCV–F9 and TV) in comparison to UV-C (254 nm) light on Formica coupons (used as a model countertop surface found in food processing and food service environments).

2. Materials and methods

2.1. Host cell lines for viral propagation

Rhesus monkey kidney epithelial cells (LLC-MK2) for the propagation of TV and Crandell- Reese Feline Kidney (CRFK) cells for the propagation of FCV-F9 were obtained from the American Type Culture Collection (Manassas, VA). Fetal rhesus monkey kidney (FRhK-4) cells for the propagation of HAV were obtained from the University of Tennessee collection. All host cells were maintained as described in earlier studies [35–37]. Briefly, LLC-MK2 cells were maintained using Opti-MEM with 2 % newborn calf serum (NCS) and 1 % Pen-strep (PS; Thermo Fisher Scientific, Pittsburgh, PA), CRFK cells were maintained with Dulbecco's Modified Eagle Medium (DMEM-F12) containing 8 % NCS and 1 % PS, while FRhK-4 cells were maintained in DMEM-F12 supplemented with 2 % NCS and 1 % PS.

2.2. Viral propagation

The viruses used in this study were propagated using published protocols and viral propagation methods are briefly summarized below [35–37].

TV was obtained as a kind gift from Dr. J. Jiang (Cincinnati Children's General Hospital, Cincinnati, OH). Confluent LLC-MK2 cells contained in sterile 175cm^2 cell-culture flasks were infected with TV and incubated at 37 °C with 5 % CO_2 for 3 h. This was followed by the addition of 10 mL of Opti-MEM containing 8 % NCS and 1 % PS and then incubated for three to five days. After observation of cytopathic effects and infectivity, the flasks were freeze thawed thrice, followed by centrifugation at 5000 rpm for 10 min and filtration through 0.2 μm filters. To increase the titer, TV stock was passed through Amicon ultra centrifugal filters (3 KDa molecular weight cut off), and centrifuged at 5000 rpm for 1 h. The filtrate containing TV was stored at −80 °C as stock for subsequent use.

FCV-F9 was purchased from ATCC (Manassas, VA). Confluent CRFK cells in sterile 175 cm^2 flasks were inoculated with FCV-F9 and incubated with 5 % CO_2 in a water-jacketed incubator at 37 °C for 3 h. Then, 10 mL DMEM with 8 % NCS and 1 % PS was added and the infected flasks were further incubated for three days until cytopathic effects were observed. The infected flasks were freeze-thawed thrice, followed by centrifugation for 10 min at 5000 rpm in the cold (4 °C) and then the supernatant was filtered through 0.2 μm filters. This filtrate was used for FCV-F9 stock and/or stored frozen at −80 °C until use.

HAV (strain HM175) was kindly provided by Dr. Kalmia Kniel's laboratory (University of Delaware). For HAV propagation, confluent FRhK-4 cells within sterile 175 cm^2 cell-culture flasks were infected with HAV and incubated at 37 °C for 3 h. Flasks were then incubated for five days in a water-jacketed incubator under 5 % CO_2 after the addition of 10 mL DMEM with 8 % NCS and 1 % PS. The infected flasks were freeze thawed three times, centrifuged, filtered through 0.2 μm filters as described above. The HAV containing filtrate was then stored frozen at −80 °C for use as the HAV stock.

2.3. UV-C LED (279 nm) treatment of viruses inoculated on Formica coupons

Sterile autoclaved Formica coupons were kept within sterile Petri dishes in a biosafety cabinet under UV-C (254 nm) light for 10 min for surface decontamination. Then, 100 μL of either TV (~7 log PFU/mL), FCV-F9 (~6 log PFU/mL), or HAV (~6 log PFU/mL), was spread onto Formica coupons (approximately 3 × 3 cm^2 area) and air-dried for 10 min (as a proof of concept) within the biosafety cabinet with one inoculated coupon for each treatment time. UV-C LED (279 nm, MD1016-1, Irtronix, Torrence, CA) treatments were then performed for up to 2.5 min for FCV using 30 s intervals (279 nm, 6.5 cm from sample, Voltage = 28.0, Ampere = 0.1, surface dose = 0–54.64 mJ/cm^2), while up to 1.25 min treatment times for TV and HAV were used.

The control (0 min) and subsequent treatments were recovered using 200 μL of DMEM with 10 % NCS and 1 % PS to elute either FCV-F9 or HAV from the inoculated Formica coupon. Ten-fold serial dilutions were then performed using DMEM containing 2 % NCS and 1 % PS. For TV, the 0 min control and treatments were recovered using 200 μL Opti-MEM containing 10 % NCS and 1 % PS initially to elute TV from the inoculated Formica coupon, and then ten-fold serial dilutions were performed with Opti-MEM containing 2 % NCS and 1 % PS. All treatments were replicated thrice and infectivity determined using plaque assays in duplicate as described below.

2.4. UV-C at 254 nm treatment of viruses inoculated on Formica coupons

Similar to the treatments with UV-LED, sterile Formica coupons were placed on sterile Petri plates under UV-C (254 nm, Labconco Purifier Class II Biosafety cabinet, Model 36,208, serial number 020421542 A) light for 10 min in a biosafety cabinet. A set of these sterile Formica coupons were then inoculated with either 100 μL of TV (~7 log PFU/mL), FCV-F9 (~6 log PFU/mL) or HAV (~6 log PFU/mL), and surface spread onto Formica coupons (approximately 3 × 3 cm^2 area) and air-dried in the biosafety cabinet for 10 min. Treatments were then performed at 30 s intervals up to 2.5 min with UV-C 254 nm hood light (254 nm, 55.88 cm/22 inches from sample, surface dose = 0–21.81 mJ/cm^2) for FCV and 1.25 min with 15 s intervals for TV and HAV. Viruses from 0 min control and treatments were recovered as reported above in section 2.3.

2.5. Infectious plaque assays

Infectivity of the control and treated viruses were determined using standard plaque assays as described before [35–37].

Briefly, host LLC-MK2 cells in six well plates were incubated at 37 °C with 5 % CO_2 until confluent, and infected with ten-fold serially diluted TV (treated and/or control). Infected plates were then incubated for 3 h at 37 °C with 5 % CO_2. Next, the media was aspirated and the cells were overlaid with 2 mL of a 1:1 ratio of 1 % Noble agar and Opti-MEM with 2 % NCS and 1 % PS. Plates were then incubated for 72 h at 37 °C with 5 % CO_2 to visualize and then enumerate plaques [36]. Plaque counts were converted to plaque forming units per mL (PFU/mL) [36,37].

Similarly, ten-fold serially diluted FCV-F9 (treated and/or control) were added to confluent host CRFK cells in six well plates and infected as described above [35,37]. Plates were then incubated at 37 °C with 5 % CO_2 for 3 h, then media were aspirated. Next, overlay media containing 2 mL of a 1:1 ratio of 1 % Noble agar and FCV-F9 2X overlay medium containing 4 % NCS, 3 % $NaHCO_3$, 2 % nonessential amino acids, 2 % L-glutamine, and 2 % penicillin-streptomycin was added. Infected plates were then incubated for 72 h at 37 °C with 5 % CO_2 prior to visualization and enumeration of plaques.

Similarly, for HAV infectivity determination, media from confluent FRhK-4 cells in six well plates were aspirated followed by the addition of ten-fold serial dilutions of 500 μL of HAV (treated and/or control) in duplicate to these plates. Infected FRhK-4 plates were then incubated at 37 °C under 5 % CO_2 for 3 h. Then, the media of the infected plates (containing treated or control dilutions) were aspirated and overlaid using 2 mL of a 1:1 ratio of 1 % Noble agar and HAV 2X overlay medium containing 4 % NCS, 3 % $NaHCO_3$, 2 % nonessential amino acids, 2 % L-glutamine, 2 % HEPES buffer, 0.2 % gentamycin-kanamycin, and 0.15 % $MgCl_2$. Plates were then incubated for 72 h at 37 °C with 5 % CO_2 prior to visualization and enumeration of plaques. All treatments were replicated thrice and assayed in duplicate as indicated above.

2.6. UV-C dose calculation

Surface dose was calculated based on product of UV intensity and exposure time in secs. The UV intensity for UV-C low pressure lamp and LED was 0.1454 mW/cm^2 and 0.36 mW/cm^2, respectively.

Surface UV-C dosage (mJ/cm^2) = UV intensity (mW/cm^2) × exposure time (secs) [38].

2.7. Statistical analysis

Each treatment time point and control treatment for each virus on Formica coupons were replicated three times and recovered infectious titers in log PFU/mL were calculated. The average per trial/replicate was analyzed using mixed model analysis of variance (MMAOV) with Tukey's adjustment ($p < 0.05$) using SAS v 9.4 (Cary, NC) and linear models were created using Excel to determine D-values [35,36].

3. Results

3.1. FCV-F9 treated with UV-C (254 nm) and UV-C LED (279 nm) on Formica coupons

Treatments of FCV-F9 on Formica coupons (Table 1) with UV-C light did not result in any significant differences in infectious titer reductions between the two tested systems, with D-values of 1.07 ± 0.04 min with UV-LED at 279 nm and 1.14 ± 0.28 min after treatments with 254 nm UV-C lamp ($p > 0.05$) without accounting for the UV intensity and UV dosage. Upon calculation of UV sensitivity (D_{10}), FCV-F9 had D_{10} values of 23.37 ± 0.91 mJ/cm^2 using 279 nm UV-C LED and 9.97 ± 2.44 mJ/cm^2 using the UV-C lamp (254 nm) on Formica coupons which were significantly different ($p < 0.05$; Table 4) from each other. It therefore remains critical to evaluate the UV sensitivity based on UV dosage and exposure time for surfaces. Herein, we have calculated the D_{10} values based on exposure time and surface UV-C dosage [38]. Perhaps the optics of the viral suspension may also play a role in varying D_{10} value, based on the viral capsid composition.

Table 1
Inactivation of FCV-F9 treated with either UV-C (254 nm) or UV-C LED (279 nm) on Formica coupons.

Time (mins)	UV-C LED System (279 nm) UV dose (mJ/cm^2)	UV-C LED System (279 nm) Reduction (log PFU/mL)	UV-C (254 nm) UV dose (mJ/cm^2)	UV-C (254 nm) Reduction (log PFU/mL)
0	0	0^{G}	0	0^{G}
0.5	10.92	0.87 ± 0.048^{EF}	4.36	0.51 ± 0.06^{FG}
1	21.84	1.36 ± 0.33^{CDE}	8.72	1.20 ± 0.21^{DE}
1.5	32.76	1.84 ± 0.09^{BC}	13.09	0.70 ± 0.15^{BCD}
2	43.68	2.07 ± 0.14^{AB}	17.45	1.86 ± 0.20^{ABC}
2.5	54.6	2.45 ± 0.05^{A}	21.81	2.26 ± 0.50^{AB}

*Capital letters denote statistically significant differences when compared across treatment times. ($p < 0.05$).
Averages of triplicate treatments ± standard deviations.

Table 2
Inactivation of TV treated with either UV-C (254 nm) or UV-C LED (279 nm) on Formica coupons.

Time (mins)	UV-C LED System (279 nm) UV dose mJ/cm^2	UV- C LED System (279 nm) Reduction (log PFU/mL)	UV-C (254 nm) UV dose mJ/cm^2	UV-C (254 nm) Reduction (log PFU/mL)
0	0	0^{E}	0	0^{E}
0.25	5.46	0.51 ± 0.20^{CDE}	2.18	0.21 ± 0.04^{DE}
0.5	10.92	0.99 ± 0.12^{BC}	4.36	0.50 ± 0.38^{CDE}
0.75	16.38	1.22 ± 0.072^{ABC}	6.54	1.03 ± 0.14^{BC}
1	21.84	0.83 ± 0.49^{BCD}	8.72	1.32 ± 0.28^{AB}
1.25	27.3	1.83 ± 0.38^{A}	10.91	1.50 ± 0.20^{AB}

*Capital letters denote statistically significant differences when compared across treatment times. ($p < 0.05$).
Averages of triplicate treatments ± standard deviations.

3.2. TV treated with UV-C (254 nm) and UV-C LED (279 nm) on Formica coupons

Similarly, TV on Formica coupons (Table 2) did not result significant differences in recovered infectious titers when treated with UV-C (254 nm) or UV-C LED (279 nm). The D-values for TV were 0.78 ± 0.13 min with 254 nm UV-C and 0.86 ± 0.21 min with the 279 nm UV-C LED system, without accounting for UV intensity and dosage ($p > 0.05$). The calculation of UV sensitivity (D_{10}) for TV resulted in D_{10} values of 16.34 ± 3.6 mJ/cm^2 with 279 nm UV-C LED and 6.83 ± 1.13 mJ/cm^2 with 254 nm UV-C on Formica coupons.

3.3. HAV treated with UV-C (254 nm) and UV-C LED (279 nm) on Formica coupons

Treatment of HAV on Formica coupons (Table 3) also did not result in significant differences in titer reductions between UV-C (254 nm) and UV-LED (279 nm) ($p > 0.05$), where HAV had D-values of 0.57 ± 0.03 min after treatment with 279 nm UV-C LED and D-values of 0.71 ± 0.07 min on Formica coupons after treatment with UV-C (254 nm). However, unlike for FCV and TV, the dosage with both systems were not significantly different for HAV ($p > 0.05$). D_{10} values of 12.39 ± 0.70 mJ/cm^2 using 279 nm UV-C LED and 12.40 ± 1.15 mJ/cm^2 with 254 nm UV-C on Formica coupons were observed.

4. Discussion

Contamination of contact surfaces and the risk of cross-contamination in the food processing environments is a significant public health issue. The resilience of foodborne viruses (including HuNoV and HAV) on contact surfaces and fomites (porous and non-porous) with the ability for survive over weeks to months depending on temperature and humidity [39–42] drive the need to implement optimal control strategies to decrease the risk of illness outbreaks. In fact, research has shown that on carpet (nylon and wool), infectious FCV survived between <1 and 15 days, while MNV-1 survived longer between 3 and 15 days [40]. TV was shown to have D-values of 18.5 ± 0.34 days and 13.1 ± 0.36 days on stainless steel and acrylic based surfaces [41]. Viral persistence studies showed that HuNoV (GI) and FCV could be detected on inoculated ceramic, stainless steel and Formica surfaces for up to 7 days [39]. Taken together, these studies highlight the role of fomites and food contact surfaces in foodborne viral disease transmission with the need for improved decontamination strategies.

Literature is currently lacking on the precise parameters needed for the application of UV-C technology for inactivation of human foodborne viruses on Formica surfaces found in the food environment. Therefore, the objective of this research study was to determine the inactivation of HAV, FCV-F9, and TV on Formica coupons (a model food contact surface) by two UV-C systems (at 254 nm and at 279 nm) for their application in real-world scenarios to decrease the risk of enteric viral disease transmission. The resistance of the historically used cultivable surrogate, FCV-F9 was compared to the relatively recent cultivable TV that has similar receptors as HuNoVs [4]. In this study, a single drying time of 10 min was used using the small 100 μL volumes of virus. It is important to note that this may not reflect all conditions experienced in the real world where viruses may be dried for longer periods on the surfaces before treatments are applied.

Table 3
Inactivation of HAV treated with either UV-C (254 nm) or UV-C LED (279 nm) on Formica coupons.

Time (min)	UV-C LED System (279 nm) UV dose mJ/cm^2	UV- C LED System (279 nm) Reduction (log PFU/mL)	UV-C (254 nm) UV dose mJ/cm^2	UV-C (254 nm) Reduction (log PFU/mL)
0	0	0^{E}	0	0^{E}
0.25	5.46	0.51 ± 0.37^{DE}	2.18	0.24 ± 0.16^{E}
0.5	10.92	1.36 ± 0.39^{BC}	4.36	0.94 ± 0.19^{CD}
0.75	16.38	1.67 ± 0.30^{AB}	6.54	1.17 ± 0.15^{BCD}
1	21.84	1.82 ± 0.32^{AB}	8.72	1.42 ± 0.17^{BC}
1.25	27.3	2.24 ± 0.22^{A}	10.91	1.72 ± 0.20^{AB}

*Capital letters denote statistically significant differences when compared across treatment times. ($p < 0.05$).
Averages of triplicate treatments ± standard deviations.

Table 4
Comparison of the D_{10} values of FCV-F9, TV and HAV treated with 254 nm UV-C and 279 nm UV-C LED on Formica coupons.

	UV-C LED System (279 nm) D_{10} value (mJ/cm^2)	UV-LED System (279 nm) D-value (min)	UV-C (254 nm) D_{10} value (mJ/cm^2)	UV-C (254 nm) D-value (min)
FCV-F9	23.37 ± 0.91^{Aa}	1.07 ± 0.04^{Ba}	9.97 ± 2.44^{Bb}	1.14 ± 0.28^{Aa}
TV	16.34 ± 3.60^{Aab}	0.86 ± 0.21^{Aab}	6.83 ± 1.13^{Bbc}	0.78 ± 0.13^{Aa}
HAV	12.39 ± 0.70^{Ac}	0.57 ± 0.03^{Bc}	12.40 ± 1.15^{Aab}	0.71 ± 0.07^{Aab}

*Capital letters denote statistically significant differences when compared across one treatment type (one row) ($p < 0.05$).
Lowercase letters denote statistically significant differences when compared down a treatment medium (one column) ($p < 0.05$).
Averages of triplicate treatments ± standard deviations; both optical devices have different UV intensities.

Using the traditional UV-C (254 nm) system, FCV-F9 had D_{10} values of 9.97 ± 2.44 mJ/cm^2, TV had D_{10} values of 6.83 ± 1.13 mJ/cm^2, and HAV had D_{10} values of 12.40 ± 1.15 mJ/cm^2 when dried on Formica coupons (Table 4). It is quite apparent that HAV and FCV showed higher resistance to UV-C at 254 nm treatments on Formica coupons than TV. UV-C technology is known to damage nucleic acids of targets and ultimately inhibit their replication [32,33], while UV-C ranging from 210 to 240 nm can damage RNA that is attributed to protein–RNA cross-linking or energy transfer from proteins to RNA and also oxidation [12,18,26]. Thus, the differences in resistance to UV-C at 254 nm between FCV, HAV and TV could be attributed to their nucleic acid sequence composition and structure as well as capsid protein size, amino acid sequence and structure including number of dimer formation. Genomes enriched with thymine/uracil will be affected significantly. The FCV-F9 capsid protein, VP1 contains 668 aa while the TV VP1 capsid contains 534 aa [43], suggesting that the length, composition, and size of the capsid could play a protective role in the resistance of FCV-F9 to treatment with UV-C at 254 nm. The VP1 capsid of HAV is reported to contain 278 aa, VP2 contains 222 aa and VP3 contains 246 aa [44], hence besides capsid size, amino acid composition and capsid protein structure (secondary and tertiary structures together with interaction with nucleic acids) can play major roles in viral stability and resistance to inactivation processes. These factors need to be further explored and also modeled in future studies.

Reports on 254 nm UV-C treatments of 50 μL MNV-1 (6.2 log PFU/mL) and HAV (5.85 log PFU/mL) dried for 1 h on stainless steel surfaces revealed a 0–4.3 log PFU/mL reduction of MNV-1 (D_{10} values of 33.3 mJ/cm^2) and 0–2.6 log PFU/mL reduction of HAV (D_{10} values of 55.4 mJ/cm^2) using doses of 10–300 mJ/cm^2 [14]. These D_{10} values were significantly higher for HAV than MNV-1 ($p < 0.05$) [14]. In our current study, both FCV-F9 (D_{10} values of 9.97 ± 2.44 mJ/cm^2) and HAV (D_{10} values of 12.40 ± 1.15 mJ/cm^2) were more resistant to UV-C treatments at 254 nm than TV (D_{10} values of 6.83 ± 1.13 mJ/cm^2) inoculated on Formica coupons. These values on Formica coupons were lower for FCV-F9 and TV than the values reported for MNV-1 on stainless steel surfaces by Park et al. [14], but show similar trends for HAV on Formica coupons (being more resistant than the HuNoV surrogates, namely TV on Formica and MNV-1 on stainless steel) to that reported for HAV on stainless steel surfaces Moreover, our results for HAV on Formica coupons (D_{10} values of 12.40 ± 1.15 mJ/cm^2, suggesting 5 log reduction with 60.2 mJ/cm^2) are comparable to the results reported using pulsed UV-C light where 60 mJ/cm^2 caused almost 5 log reduction of HAV on stainless steel and PVC surfaces [16,17].

Earlier research used a 30 W UV (with 10 W output) at 253.4 nm lamp showed higher resistance of FCV-F9 than HAV, where 1–3 mL of FCV-F9 and HAV suspended into PBS onto a Petri dish resulted in a >2 log PFU/mL reduction of FCV-F9 and a >4 log PFU/mL reduction of HAV with doses of 125 mJ/cm^2 [21]. In our study using Formica coupons, HAV showed 1.42 log reduction after 1 min (dosage of 17.45 mJ/cm^2), while FCV-F9 showed 1.2 log reduction after 1 min (dosage of 8.72 mJ/cm^2) using UV-C at 254 nm. Other studies showed that TV was reduced by > 4 log using 254 nm UV-C at 60–70 mJ/cm^2 when 250 μL was placed into 6 well plates [4]. In our study with treatments of UV-C at 254 nm, TV had D_{10} values of 6.83 ± 1.13 mJ/cm^2 on Formica coupons (suggesting 4 log PFU reduction using ~28 mJ/cm^2). The differences between studies can be attributed due to the different matrices and methods (PBS in petridishes versus drying on Formica coupons) used, varying treatment conditions and potentially also the non-uniform UV dose exposure conditions.

As mentioned above, literature is currently lacking on the effects of UV-C LED at 279 nm against foodborne viruses. Though, UV-C LED has been successfully applied to inactivate aerosolized bacteriophages, bacteria, and fungi, where bacteria were reported to be the most sensitive to UV-C LED among the tested microorganisms, while bacteriophages MS2, Qβ, and ΦX174 (7–8 log PFU/27 L) were inactivated by 5 log PFU/27 L after treatment with 45 mJ/cm^2 for up to 10 min [28]. UV-C LED is known to converge linearly unlike UV lamps whose lights scatters, which may decrease the strength of the intensity [45]. In the current study, FCV-F9 inoculated and surface spread on Formica coupons was most resistant to UV-C LED at 279 nm treatment, among the three tested viruses, with a D_{10} value of 23.37 mJ/cm^2 followed by TV with a D_{10} value of 16.34 mJ/cm^2, and then HAV with a D_{10} value of 12.39 mJ/cm^2.

When comparing the two UV-C systems used for the inactivation of the three tested viruses, HAV showed similar inactivation at UV-C at 254 nm to UV-C at 279 nm (requiring similar doses for inactivation by both systems ($p > 0.05$)). However, both FCV-F9 and TV were more sensitive to UV-C at 254 nm requiring lower doses for inactivation than using UV-C LED at 279 nm. However, the advantages of UV-C LED at 279 nm with the relatively lower risk to handlers and users and lower environmental hazards, make this technology a promising alternative novel UV-C inactivation option. Overall, the reported studies with UV-C suggest that using alternate UV-C systems to UV-C mercury lamps and at alternate wavelengths provide improved ways to inactivate pathogens in the food environment. It is important to keep in mind that at least a 6 log reduction for food safety applications has been recommended [46].

As reported earlier, UV-C at 279 nm theoretically damages proteins and protein-RNA structures [34]. In addition to nucleic acid content, the capsid protein-RNA interaction, folding and structure could play key roles in resistance or susceptibility to UV-C treatments. The pI of the VP1 capsid protein that is linked to the amino acid composition of TV is at a pH of 10 [43], for HAV at pH of 7.15 [47], at a pH of 4.27 for FCV-F9 (Mayer et al., 2015), and at a pH of 4.65 for HuNoV [48]. These differences in protein properties and their potential differences in protein-RNA complex formation could account for the higher resistance of FCV-F9 to treatments with UV-C LED at 279 nm. Hence, depending on the optimal wavelength of treatment, the properties of the virus in terms of protein structure and composition and RNA structure and composition contribute to its resistance to UV-C treatments. As an example, the positive-sense, single stranded-RNA bacteriophage MS2 (non-enveloped virus) that has been used as a surrogate for foodborne viruses and as an indicator for UV reactor validation in the US, could be inactivated using <300 nm wavelengths [12,49]. However, its inactivation was reported to increase three times using 214 nm compared to inactivation at 254 nm [49].

Thus, UV-LED at 279 nm shows promise for surface decontamination of HAV and the tested HuNoV surrogates when air-dried on Formica coupons for 10 min. A single short drying time of 10 min was used in this study, and is a limitation where longer drying times need to be explored. In addition, further testing with the cultivable HuNoVs will help establish the precise UV-C dosage needed for inactivation to prevent outbreaks. However, as mentioned earlier, high HuNoV titers are needed to observe and enumerate >3 log reduction during experimentation. Additionally, testing on porous surfaces may provide data to increase the utility of UV-C LED systems in a wide range of settings including clinical and agricultural environments.

From literature and the results of our current study, UV-C LED remains a growing area of research interest due to the mercury free design, durability, and lack of warm up time [23,28]. Besides, there is potential for the inactivation of aerosolized viruses, bacteria and fungal pathogens (both foodborne and respiratory) and also toxins that could be found on the surfaces of food processing environments, in clinical settings and in food systems themselves using these novel UV-C LED systems.

5. Conclusions

This research shows that UV-C LED (279 nm) is a promising user-friendly technology for the inactivation of HAV and the tested HuNoV surrogates when dried for 10 min on Formica coupons as model contact surfaces. While the targeted viruses when dried for 10 min on Formica coupons were also inactivated by UV-C at 254 nm, further drying times need to be tested using both UV-C systems. These UV-C dose response data will be useful to implement optimal UV-C control strategies to decrease foodborne viral contamination and reduce the risk of cross-contamination events to prevent and control foodborne viral outbreaks. Furthermore, it remains critical to incorporate the suspension media optical data and adjust/calculate the delivered UV-C dosages for virus kinetic studies. These data also show promise for further testing of UV-C systems for foodborne virus inactivation in fluid foods.

CRediT authorship contribution statement

E.Corson nee Camfield: Writing – original draft, Methodology, Formal analysis. **B. Pendyala:** Writing – review & editing, Formal analysis. **A. Patras:** Writing – review & editing, Project administration, Funding acquisition, Conceptualization. **D.H. D'Souza:** Writing – review & editing, Supervision, Project administration, Investigation, Funding acquisition, Conceptualization.

Declaration of competing interest

The authors declare the following financial interests/personal relationships which may be considered as potential competing interests: Authors report that financial support was provided by USDA National Institute of Food and Agriculture.

Acknowledgements

The authors gratefully acknowledge the funding provided by USDA AFRI grant # 2019–69015-29233 for this research study. This research appears as part of a chapter of the Master's thesis of Emily Corson nee Camfield in partial fulfilment of her MS degree at the University of Tennessee, Knoxville [50].

References

[1] CDC, Multistate Outbreak of Hepatitis A Virus Infections Linked to Frozen Organic Strawberries, 2023. https://www.cdc.gov/hepatitis/outbreaks/2023/hav-contaminatedfood/index.htm#:~:text=Traceback%20and%20epidemiological%20investigations%20show,been%20reported%20from%202%20states.
[2] CDC, Mutistate norovirus outbreak linked to raw oysters from Texas, Updated April, 14, 2023, https://www.cdc.gov/norovirus/outbreaks/index.html, 2023.
[3] CDC, Norovirus | norovirus worldwide | CDC. https://www.cdc.gov/norovirus/trends-outbreaks/worldwide.html, 2020. (Accessed 8 October 2020).
[4] P. Tian, D. Yang, C. Quigley, M. Chou, X. Jiang, Inactivation of the Tulane virus, a novel surrogate for the human norovirus, J. Food Protect. 76 (4) (2013) 712–718, https://doi.org/10.4315/0362-028X.JFP-12-361.
[5] M.K. Estes, K. Ettayebi, V.R. Tenge, K. Murakami, U. Karandikar, S.-C. Lin, V.B. Ayyar, Human norovirus cultivation in nontransformed stem cell-derived human intestinal enteroid cultures: success and challenges, Viruses 11 (7) (2019) 638, https://doi.org/10.3390/v11070638.
[6] K. Ettayebi, V.R. Tenge, N.W. Cortes-Penfield, S.E. Crawford, F.H. Neill, X.L. Zeng, X. Yu, B.V. Ayyar, D. Burrin, S. Ramani, R.L. Atmar, M.K. Estes, New insights and enhanced human norovirus cultivation in human intestinal enteroids, mSphere 6 (1) (2021) e01136, https://doi.org/10.1128/mSphere.01136-20. PMID: 33504663; PMCID:PMC788532.

[7] K. Ettayebi, S.E. Crawford, K. Murakami, J.R. Broughman, U. Karandikar, V.R. Tenge, F.H. Neill, S.E. Blutt., X.-L. Zeng, L. Qu, B. Kou, A.R. Opekun, D. Burrin, D. Y. Graham, S. Ramani, R.L. Atmar, M.K. Estes, Replication of human noroviruses in stem cell-derived human enteroids, Science 353 (6306) (2016) 1387–1393, https://doi.org/10.1126/science.aaf5211.

[8] WHO, "WHO | Hepatitis A." WHO, World Health Organization, 2015. http://www.who.int/immunization/diseases/hepatitisA/en/.

[9] A. Patras, M.S. Bhullar, B. Pendyala, F. Crapulli, UV treatment of opaque liquid foods: from theory to practice, in: K. Muthukumarappan, K. Knoerzer (Eds.), Innovative Food Processing Technologies: A Comprehensive Review, 2. Elsevier Reference Modules, 2020, pp. 182–209.

[10] P. Vashisht, B. Pendyala, A. Patras, V. Gopisetty, R. Ravi, Design and efficiency evaluation of a mid-size serpentine Dean flow UV-C system for the processing of whole milk using computational fluid dynamics and biodosimetry, J. Food Eng. 335 (111168) (2022). ISSN 0260-8774.

[11] FDA, Center for Devices and Radiological Health. UV Lights and Lamps: Ultraviolet-C Radiation, Disinfection, and Coronavirus, FDA, August, 2020.

[12] H. Ezzatpanah, V.M. Gómez-López, T. Koutchma, F. Lavafpour, F. Moerman, M. Mohammadi, D. Raheem, New food safety challenges of viral contamination from a global perspective: conventional, emerging, and novel methods of viral control, Compr. Rev. Food Sci. Food Saf. 21 (2) (2022) 904–941, https://doi.org/10.1111/1541-4337.12909. Epub 2022 Feb 12. PMID: 35156303.

[13] J.A. Guerrero-Beltran, G.V. Barbosa-Canovas, Review: advantages and limitations on processing foods by UV light, Food Sci. Technol. Int. 10 (3) (2004) 137–147.

[14] S.Y. Park, A.-N. Kim, K.-H. Lee, S.-D. Ha, Ultraviolet-C efficacy against a norovirus surrogate and hepatitis A virus on a stainless steel surface, Int. J. Food Microbiol. 211 (October) (2015) 73–78, https://doi.org/10.1016/j.ijfoodmicro.2015.07.006.

[15] D. Li, L. Baert, M. De Jonghe, E. Van Coillie, J. Ryckeboer, F. Devlieghere, M. Uyttendaele, Inactivation of murine norovirus 1, coliphage phiX174, and Bacteroides [corrected] fragilis phage B40-8 on surfaces and fresh-cut iceberg lettuce by hydrogen peroxide and UV light, Appl. Environ. Microbiol. 77 (4) (2011) 1399–1404, https://doi.org/10.1128/AEM.02131-10. Epub 2010 Dec 23. Erratum in: Applied and Environmental Microbiology, 2011 Mar;77(6):2200. PMID: 21183630; PMCID: PMC3067203.

[16] J. Jean, R. Morales-Rayas, M.-N. Anoman, S. Lamhoujeb, Inactivation of hepatitis A virus and norovirus surrogate in suspension and on food-contact surfaces using pulsed UV light (pulsed light inactivation of food-borne viruses), Food Microbiol. 28 (3) (2011) 568–572, https://doi.org/10.1016/j.fm.2010.11.012.

[17] A. Vimont, I. Fliss, J. Jean, Efficacy and mechanisms of murine norovirus inhibition by pulsed-light technology, Appl. Environ. Microbiol. 81 (8) (2015) 2950–2957, https://doi.org/10.1128/AEM.03840-14.

[18] V.M. Gómez-López, E. Jubinville, M.I. Rodríguez-López, M. Trudel-Ferland, S. Bouchard, J. Jean, Inactivation of foodborne viruses by UV light: a review, Foods 10 (12) (2021) 3141, https://doi.org/10.3390/foods10123141.

[19] R. Choudhary, S. Bandla, Ultraviolet pasteurization for food industry, Int. J. food Sci. Nutrit. Eng. 2 (1) (2012) 12–15, https://doi.org/10.5923/j.food.20120201.03, p-ISSN: 2166-5168 e-ISSN: 2166-5192.

[20] G.W. Park, K.G. Linden, M.D. Sobsey, Inactivation of murine norovirus, feline calicivirus and echovirus 12 as surrogates for human norovirus (NoV) and coliphage (F+) MS2 by ultraviolet light (254 Nm) and the effect of cell association on UV inactivation, Lett. Appl. Microbiol. 52 (2) (2011) 162–167, https://doi.org/10.1111/j.1472-765X.2010.02982.x.

[21] S. Nuanualsuwan, T. Mariam, S. Himathongkham, D.O. Cliver, Ultraviolet inactivation of feline calicivirus, human enteric viruses and coliphages, Photochem. Photobiol. 76 (4) (2002) 40610, https://doi.org/10.1562/00318655(2002)0760406UIOFCH2.0.CO2.

[22] J. Chen, S. Loeb, J.-K. Kim, LED revolution: fundamentals and prospects for UV disinfection applications, Environ. Sci. J. Integr. Environ. Res.: Water Res. Technol. 3 (2) (2017) 188–202, https://doi.org/10.1039/C6EW00241B.

[23] K. Song, M. Mohseni, F. Taghipour, Application of ultraviolet light-emitting diodes (UV-LEDs) for water disinfection: a review, Water Res. 94 (May) (2016) 341–349, https://doi.org/10.1016/j.watres.2016.03.003.

[24] A. Kheyrandish, M. Mohseni, F. Taghipour, Protocol for determining ultraviolet light emitting diode (UV-LED) fluence for microbial inactivation studies, Environ. Sci. Technol. 52 (13) (2018) 7390–7398, https://doi.org/10.1021/acs.est.7b05797.

[25] L. Nyhan, M. Przyjalgowski, L. Lewis, M. Begley, M. Callanan, Investigating the use of ultraviolet light emitting diodes (UV-LEDs) for the inactivation of bacteria in powdered food ingredients, Foods 10 (4) (2021) 797, https://doi.org/10.3390/foods10040797.

[26] C. Pihen, Emma Mani-López, Avelina Franco-Vega, M.T. Jiménez-Munguía, A. López-Malo, N. Ramírez-Corona, Performance of UV-LED and UV-C treatments for the inactivation of Escherichia coli ATCC 25922 in food model solutions: influence of optical and physical sample characteristics, Innovat. Food Sci. Emerg. Technol. 85 (2023) 103314.

[27] C. Lee, K.H. Park, M. Kim, Y.B. Kim, Optimized parameters for effective SARS-CoV-2 inactivation using UVC-LED at 275 nm, Science Reports 12 (1) (2022) 16664, https://doi.org/10.1038/s41598022-20813-4.

[28] D.-K. Kim, D.-H. Kang, UVC LED irradiation effectively inactivates aerosolized viruses, bacteria, and fungi in a chamber-type air disinfection system, Appl. Environ. Microbiol. 84 (17) (2018) e00944, https://doi.org/10.1128/AEM.00944-18.

[29] R.K. Maguluri, P. Nettam, S.R. Chaudhari, S.K. Yannam, Evaluation of UV-C LEDs efficacy for microbial inactivation in tender coconut water, J. Food Process. Preserv. (2021), https://doi.org/10.1111/jfpp.15727.

[30] G. Baykus, M.P. Akgun, Unlutlurk, Effects of ultraviolet-light emitting diodes (UV-LEDs) on microbial inactivation and quality attributes of mixed beverage made from blend of carrot, carob, ginger, grape and lemon juice, Innovat. Food Sci. Emerg. Technol. 67 (January) (2021) 10257285.

[31] M.S. Bhullar, A. Patras, A. Kilonzo-Nthenge, B. Pokharel, M. Sasges, Ultraviolet inactivation of bacteria and model viruses in coconut water using a collimated beam system, Food Sci. Technol. Int. 25 (7) (2019) 562–572, https://doi.org/10.1177/1082013219843395.

[32] A. Ariza-Mateos, S. Prieto-Vega, R. Díaz-Toledano, A. Birk, H. Szeto, I. Mena, A. Berzal-Herranz, J. Gómez, RNA self-cleavage activated by ultraviolet light-induced oxidation, Nucleic Acids Res. 40 (4) (2012) 1748–1766, https://doi.org/10.1093/nar/gkr822.

[33] T. Dai, M.S. Vrahas, C.K. Murray, M.R. Hamblin, Ultraviolet C irradiation: an alternative antimicrobial approach to localized infections? Expert Rev. Anti-Infect. Therapy 10 (2) (2012) 185–195, https://doi.org/10.1586/eri.11.166.

[34] E. Araud, M. Fuzawa, J.L. Shisler, J. Li, T.H. Nguyen, UV inactivation of rotavirus and Tulane virus targets different components of the virions, Appl. Environ. Microbiol. 86 (4) (2020) e02436, https://doi.org/10.1128/AEM.02436-19. PMID:31811032; PMCID: PMC6997730.

[35] S.S. Joshi, L. Dice, S. Ailavadi, D.H. D'Souza, Antiviral effects of quillaja Saponaria extracts against human noroviral surrogates, Food Environ. Virol. 15 (2023), https://doi.org/10.1007/s12560-023-09550-7. Epub ahead of print. PMID: 36920726.

[36] S. Ailavadi, P.M. Davidson, M.T. Morgan, D.H. D'Souza, Thermal inactivation kinetics of Tulane virus in cell-culture medium and spinach, J. Food Sci. 84 (3) (2019) 557–563, https://doi.org/10.1111/1750-3841.14461.

[37] X. Su, D.H. D'Souza, Grape seed extract for foodborne virus reduction on produce, Food Microbiol. 34 (1) (2013) 1–6, https://doi.org/10.1016/j.fm.2012.10.006.

[38] G. Baldelli, M.P. Aliano, G. Amagliani, M. Magnani, G. Brandi, C. Pennino, G.F. Schiavano, Airborne microorganism inactivation by a UV-C LED and ionizer-based continuous sanitation air (CSA) system in train environments, Int. J. Environ. Res. Publ. Health 19 (3) (2022) 1559, https://doi.org/10.3390/ijerph19031559.

[39] D.H. D'Souza, A. Sair, K. Williams, E. Papafragkou, J. Jean, C. Moore, L. Jaykus, Persistence of caliciviruses on environmental surfaces and their transfer to food, Int. J. Food Microbiol. 108 (1) (2006) 84–91, https://doi.org/10.1016/j.ijfoodmicro.2005.10.024. Epub 2006 Feb 13. PMID: 16473426.

[40] D. Buckley, A. Fraser, G. Huang, X. Jiang, Recovery optimization and survival of the human norovirus surrogates feline calicivirus and murine norovirus on carpet, Appl. Environ. Microbiol. 83 (22) (2017) e01336, https://doi.org/10.1128/AEM.01336-17.

[41] S.E. Arthur, K.E. Gibson, Environmental persistence of Tulane virus - a surrogate for human norovirus, Can. J. Microbiol. 62 (5) (2016) 449–454, https://doi.org/10.1139/cjm-2015-0756. Epub 2015 Dec 15. PMID: 26825139.

[42] R.A. Canales, K.A. Reynolds, A.M. Wilson, S.L.M. Fankem, M.H. Weir, J.B. Rose, S. Abd Elmaksoud, C.P. Gerba, Modeling the role of fomites in a norovirus outbreak, J. Occup. Environ. Hyg. 16 (1) (2019) 16–26, https://doi.org/10.1080/15459624.2018.1531131. PMID: 30274562.

[43] T. Farkas, K. Sestak, C. Wei, X. Jiang, Characterization of a rhesus monkeycalicivirus representing a new genus of Caliciviridae, J. Virol. 82 (11) (2008) 5416, https://doi.org/10.1128/JVI.00070-08. Epub 2008 Apr 2. PMID: 18385231;PMCID: PMC239520.

[44] D.I. Stuart, J. Ren, X. Wang, Z. Rao, E.E. Fry, Hepatitis A virus capsid structure, Cold Spring Harbor Perspect. Medi. 9 (5) (2019), https://doi.org/10.1101/cshperspect.a031807.
[45] S.-J. Kim, D.-K. Kim, D.-H. Kang, Using UVC light-emitting diodes at wavelengths of 266 to 279 nanometers to inactivate foodborne pathogens and pasteurize sliced cheese, Appl. Environ. Microbiol. 82 (1) (2016) 11–17, https://doi.org/10.1128/AEM.02092-15.
[46] FDA, Hazard Analysis and Risk-Based Preventive Controls for Human Food: Draft Guidance for Industry1, 2018. https://www.fda.gov/media/99572/download. (Accessed 1 March 2020).
[47] M. Weitz, B.M. Baroudy, W.L. Maloy, J.R. Ticehurst, R.H. Purcell, Detection of a genome-linked protein (VPg) of hepatitis A virus and its comparison with other picornaviral VPgs, J. Virol. 60 (1) (1986) 124–130.
[48] B.K. Mayer, Y. Yang, D.W. Gerrity, M. Abbaszadegan, The impact of capsid proteins on virus removal and inactivation during water treatment processes, Microbiol. Insights 8s2 (January) (2015) S31441, https://doi.org/10.4137/MBI.S31441.
[49] H. Mamane-Gravetz, K.G. Linden, A. Cabaj, R. Sommer, Spectral sensitivity of bacillus subtilis spores and MS2 coliphage for validation testing of ultraviolet reactors for water disinfection, Environ. Sci. Technol. 39 (20) (2005) 7845–7852, https://doi.org/10.1021/es048446t.
[50] E. Camfield, M.S. Thesis. Inactivation of Hepatitis A Virus and Norovirus by Heat and Ultraviolet Light: Surrogates for Validation in Food Processing Applications, M.S. thesis, UT Trace, 2021.